

Two-dimensional electron gas in Zn-polar ZnMgO/ZnO heterostructure grown by metal-organic vapor phase epitaxy

J. D. Ye,^{1,a),b)} S. Pannirselvam,² S. T. Lim,² J. F. Bi,² X. W. Sun,³ G. Q. Lo,¹ and K. L. Teo^{2,a)}

¹*Institute of Microelectronics, 11 Science Park Road, Singapore 117685*

²*Department of Electrical and Computer Engineering, National University of Singapore, Singapore 117576*

³*School of Electrical and Electronic Engineering, Nanyang Technological University, Singapore 639798*

(Received 21 July 2010; accepted 22 August 2010; published online 15 September 2010)

We report the formation of two-dimensional electron gas (2DEG) at the $\text{Zn}_{1-x}\text{Mg}_x\text{O}/\text{ZnO}$ interface grown by metal-organic vapor phase epitaxy on sapphire substrates. The existence of the 2DEG is confirmed by the observation of Shubnikov–de Haas oscillations and the integer quantum Hall effect. In particular, the $\text{Zn}_{0.8}\text{Mg}_{0.2}\text{O}/\text{ZnO}$ heterostructure shows a high Hall mobility of $2138 \text{ cm}^2/\text{V s}$ with a carrier sheet density of $3.51 \times 10^{12} \text{ cm}^{-2}$ at 1.4 K. We attribute the origin of 2DEG to be the donor states on ZnMgO surface. The dependence of carrier sheet density of 2DEG on ZnMgO layer thickness and Mg composition (x) are also investigated. © 2010 American Institute of Physics. [doi:10.1063/1.3489101]

Since the observation of Shubnikov–de Haas (SdH) oscillations and the quantum Hall effect (QHE) in high mobility two-dimensional electron gas (2DEG) in polar $\text{ZnO}/\text{Zn}_{1-x}\text{Mg}_x\text{O}$ heterostructures,¹ there is a considerable interest in the utilization of polarization field in polar oxide based heterostructure epitaxy. So far, the formation of 2DEG at the $\text{Zn}_{1-x}\text{Mg}_x\text{O}/\text{ZnO}$ interface has been observed only by a few groups using either molecular beam epitaxy (MBE) or pulse laser deposition techniques.^{2–7} On the other hand, metal-organic vapor phase epitaxy (MOVPE) is well known to be one of the most important deposition processes for making high-quality epilayers and well-defined heterostructure with homogeneous properties over a large deposition area. In this work, we report the formation of 2DEG confined in Zn-polar $\text{Zn}_{1-x}\text{Mg}_x\text{O}/\text{ZnO}$ heterostructure which can be realized by the MOVPE technique. The formation mechanism and transport properties of 2DEG are also discussed on the basis of a simple charge control model that utilizes the effect of polarization-induced charge density.

$\text{Zn}_{1-x}\text{Mg}_x\text{O}/\text{ZnO}$ heterostructures were grown on sapphire (0001) substrates using Aixtron MOVPE system with close-coupled showerhead (CCS) configuration. Dimethylzinc (DMZn) and bis(methylcyclopentadienyl) magnesium (MeCp_2Mg) were used as Zn and Mg sources, respectively. We used the nitrous oxide (N_2O) as the oxidizing source and nitrogen gas as the carrier gas. After annealing the substrate in N_2 at 1000°C , a $0.4\text{-}\mu\text{m}$ -thick ZnO buffer layer was deposited at 450°C , followed by a $3.3\text{ }\mu\text{m}$ undoped ZnO layer and an undoped $\text{Zn}_{1-x}\text{Mg}_x\text{O}$ layer, both grown at 920°C . We note that the deposited ZnO layer exhibits a Zn-face polarity with excellent crystal quality and layer-by-layer surface morphology.⁸ A series of $\text{Zn}_{1-x}\text{Mg}_x\text{O}$ layer with different thickness ranging from 27 to 120 nm was also grown under same conditions. The Mg composition (x) was determined from the reflectance measurement of the band

gap energy of $\text{Zn}_{1-x}\text{Mg}_x\text{O}$ and using the equation $E_g(x) = E_g(0) + 2.145x$.⁹ The capacitance-voltage (C-V) measurement was performed using mercury contacts at frequency of 1 MHz. The Hall effect and magnetotransport were carried out using a van der Pauw configuration with a magnetic field up to 10 T at 1.4 K.

Figure 1 shows a typical atomic force microscopy (AFM) image of $\text{Zn}_{0.83}\text{Mg}_{0.17}\text{O}$ epilayer with thickness of 27 nm. The growth condition is optimized in order to obtain a two-dimensional layer-by-layer epitaxial mode for the Zn-polar $\text{Zn}_{1-x}\text{Mg}_x\text{O}$ layer. We observe the surface morphology is dominated by wide terrace features with surface rms roughness of $\sim 0.23 \text{ nm}$. Figure 2 shows the asymmetric reciprocal space map of (105) plane measured by high-resolution x-ray diffraction. Both the ZnO and $\text{Zn}_{0.83}\text{Mg}_{0.17}\text{O}$ peaks are located at the same position of Q_x , the reciprocal space vector in the plane of the layers. This feature suggested

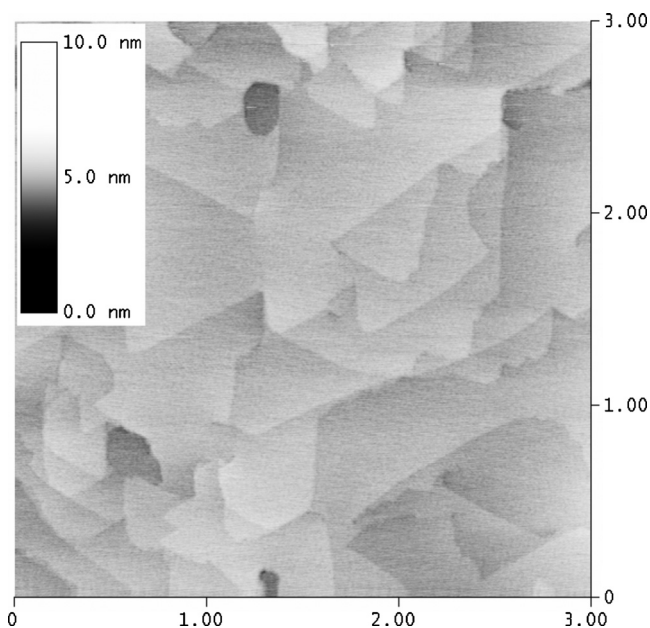


FIG. 1. AFM image of $\text{Zn}_{0.83}\text{Mg}_{0.17}\text{O}$ epilayer with thickness of 27 nm on ZnO template.

^{a)}Authors to whom correspondence should be addressed. Electronic addresses: jiangong.ye@anu.edu.au and eleteokl@nus.edu.sg.

^{b)}Present address: Department of Electronic Materials Engineering, Australian National University, Acton, 0200 Canberra, Australia.

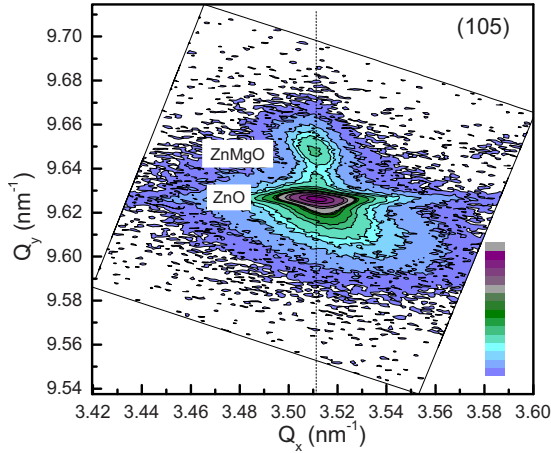


FIG. 2. (Color online) Reciprocal lattice mapping of (105) plane of $\text{Zn}_{0.83}\text{Mg}_{0.17}\text{O}/\text{ZnO}$ heterostructure. The intensity contours are illuminated in log-scale.

that the $\text{Zn}_{0.83}\text{Mg}_{0.17}\text{O}$ layer is coherently strained to the underneath ZnO layer.

Figure 3 displays the typical C-V concentration profile as a function of distance from the top surface for the $\text{Zn}_{0.83}\text{Mg}_{0.17}\text{O}/\text{ZnO}$ heterostructure. The high electron concentration observed is the confined 2DEG at the interface. As we move away from the interface, the net donor density falls off sharply, reaching a value of $1.5 \times 10^{16} \text{ cm}^{-3}$ at the ZnO layer. The dip of carrier concentration in the depth-profiling at $0.125 \mu\text{m}$ is due to the undoped ZnO grown under the conditions of lower rate and higher V/III ratio. The integration of area under the accumulation peak of the $\text{Zn}_{0.83}\text{Mg}_{0.17}\text{O}/\text{ZnO}$ interface yields a sheet concentration of $1.23 \times 10^{12} \text{ cm}^{-2}$ for the 2DEG. We found that the sheet carrier concentration increases with the ZnMgO layer thickness as well as the x composition. This behavior is similar to the case in 2DEG at AlGaIn/GaN heterostructure, in which strong electric polarization effects lead to the formation of high carrier concentration.^{10–13} The formation mechanism of 2DEG will be discussed from the viewpoint of polarization effects later.

Figures 4 show the magnetoresistance (R_{xx}) and Hall resistance (R_{xy}) as a function of magnetic field (B) up to 10 T at 1.4 K for the $\text{Zn}_{0.83}\text{Mg}_{0.17}\text{O}/\text{ZnO}$ heterostructure. In the magnetoresistance, strong SdH oscillations are clearly seen and the 2DEG density is estimated by the oscillation period

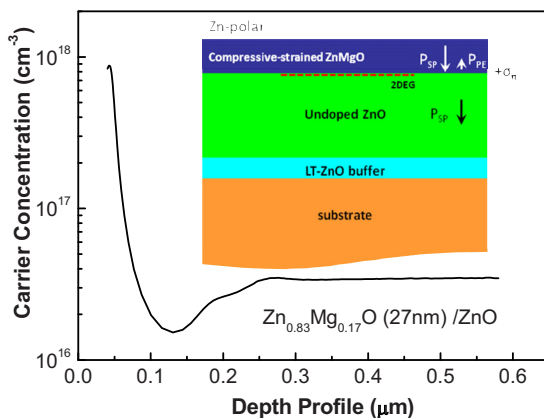


FIG. 3. (Color online) C-V depth profiling of the 2DEG and net donor concentration in $\text{Zn}_{0.83}\text{Mg}_{0.17}\text{O}/\text{ZnO}$ heterostructure. The inset shows the schematic diagram of ZnMgO/ZnO heterostructure.

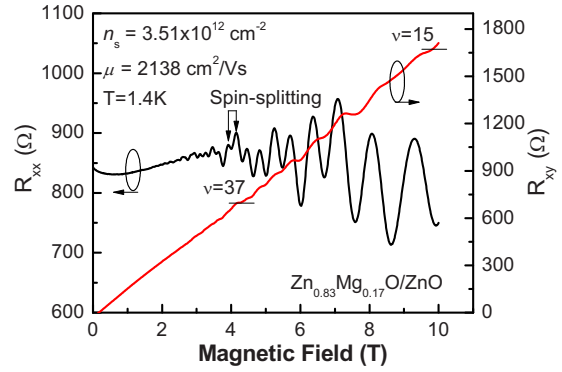


FIG. 4. (Color online) Magnetic field (B) dependence of magnetoresistance (R_{xx}) and quantum Hall resistance (R_{xy}) for $\text{Zn}_{0.83}\text{Mg}_{0.17}\text{O}/\text{ZnO}$ heterostructure measured at 1.4 K. The arrows indicate the spin-splitting in 2DEG.

to be $\sim 1.91 \times 10^{12} \text{ cm}^{-2}$. The observation of the QHE effect gives direct evidence of the existence of a 2DEG at the ZnMgO/ZnO heterostructure interface. The onset of SdH oscillations occurs at a B field of 3 T and the spin splitting of the Landau levels is visible at filling factors as high as $\nu=37$. The electron density was determined to be $n_H=3.51 \times 10^{12} \text{ cm}^{-2}$ from the low-field Hall resistivity and its corresponding mobility is $2138 \text{ cm}^2/\text{V s}$. The discrepancy in the sheet density determination from the magnetoresistance and Hall effect could be due to the significant parallel conduction in our sample. Additionally, the minima in R_{xx} do not approach zero in the integer QHE states. We believe that the parallel conduction path is originated from the interfacial layer of ZnO and sapphire, which suffered from a large dislocation density and Al donor diffusion from sapphire substrate during the high temperature epitaxial growth. This parallel conduction results in the underestimation of Hall mobility of 2DEG at the ZnMgO/ZnO interface.

In order to understand the behavior of 2DEG density as a function of $\text{Zn}_{1-x}\text{Mg}_x\text{O}$ layer thickness and x composition, we need to consider the mechanisms that control the transfer of electrons in the $\text{Zn}_{1-x}\text{Mg}_x\text{O}/\text{ZnO}$ system. We make use of a simple charge control model to calculate the 2DEG sheet carrier concentration and then compare with our work and those reported in the literature. In the absence of the external field, the total polarization of ZnO or $\text{Zn}_{1-x}\text{Mg}_x\text{O}$ layers is the sum of the spontaneous polarization (P_{SP}) and the strain-induced piezoelectric polarization (P_{PE}), and their directions are indicated in the inset of Fig. 3.

We assume that the $\text{Zn}_{1-x}\text{Mg}_x\text{O}$ layer is fully strained on ZnO and polarization constants vary linearly with x composition. Thus, the dependence of total polarizations induced charges on the x composition in $\text{Zn}_{1-x}\text{Mg}_x\text{O}$ barrier can be expressed as $\sigma(x)=0.029x \text{ (C/m}^2\text{)}$.⁹ Since the surface of the grown $\text{Zn}_{1-x}\text{Mg}_x\text{O}/\text{ZnO}$ is Zn-polar, the positive polarization-induced charges are located at the interface (see inset of Fig. 3). These positive charges tend to be compensated by the electrons that formed a 2DEG at the $\text{Zn}_{1-x}\text{Mg}_x\text{O}/\text{ZnO}$ interface. The maximum sheet carrier concentration (n_s) located at this interface of the nominally undoped structure can be expressed as^{11,12,15}

$$n_s(x) = \frac{+\sigma(x)}{e} - \left[\frac{\epsilon_0 \epsilon(x)}{de^2} \right] [e\phi_b(x) + E_F(x) - \Delta E_C(x)], \quad (1)$$

where d is the width of the ZnMgO layer thickness and x is the Mg content. The surface potential $e\phi_b(x)$ is assumed to

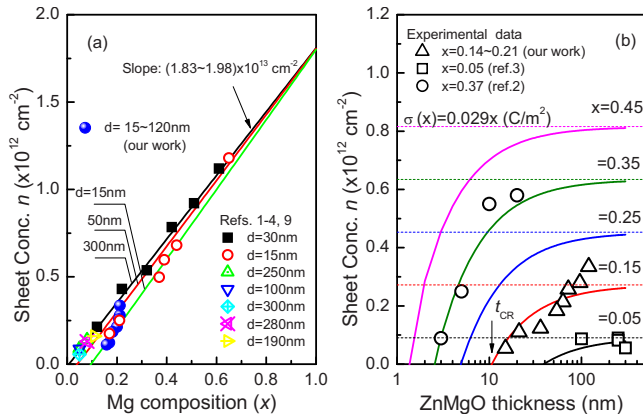


FIG. 5. (Color online) The dependence of sheet carrier concentration n as a function of (a) Mg composition (x) and (b) $\text{Zn}_{1-x}\text{Mg}_x\text{O}$ layer thickness. The solid lines correspond to the calculated results based on Eq. (1).

be pinned at surface with a level of 0.8 eV below ZnO conduction band edge and the conduction band offset ΔE_C is given as $0.9 \times \Delta E_g$.¹⁶ We approximate the Fermi level E_F by the infinite triangular quantum well,¹² which can be expressed as

$$E_F(x) = \left[\frac{9\pi\hbar e^2}{8\varepsilon_0\sqrt{8m^*}} \frac{n_S(x)}{\varepsilon(x)} \right]^{2/3} + \frac{\pi\hbar^2}{m^*} n_S(x), \quad (2)$$

where the effective mass is taken to be $m^* \approx 0.26m_e$ and the dielectric constant is approximated to be linearly dependent on x ; $\varepsilon(x) = 8.75 + 1.08x$.⁹ By substituting the required values in Eq. (1), the maximum n_S can be determined.

Figure 5(a) shows the sheet carrier concentrations (n) as a function of x composition for different $\text{Zn}_{1-x}\text{Mg}_x\text{O}$ layer thickness. The solid lines correspond to the calculated results based on Eq. (1) for $d = 15, 50,$ and 300 nm. The 2DEG density is seen to increase approximately linearly with x and the slope shows a very slight variation of $(1.83-1.98) \times 10^{13} \text{ cm}^{-2}$ indicating that the dependence on the $\text{Zn}_{1-x}\text{Mg}_x\text{O}$ layer thickness is small. This trend is very similar to those observed in O-polar or Zn-polar $\text{Zn}_{1-x}\text{Mg}_x\text{O}/\text{ZnO}$ structures grown by MBE.^{2,14} The calculated 2DEG density agrees well with our experimental results and also those reported in the literature obtained either by C-V profiling or low temperature Hall measurements.^{1-4,9,14} Figure 5(b) shows the dependence of sheet carrier concentration (n) as a function of $\text{Zn}_{1-x}\text{Mg}_x\text{O}$ layer thickness for different x . The solid lines correspond to the calculated results based on Eq. (1) for various x . As the $\text{Zn}_{1-x}\text{Mg}_x\text{O}$ layer thickness increases, the 2DEG density approaches the maximum value of polarization-induced sheet charge density $\sigma(x)$ as indicated by dashed lines in Fig. 5(b). The charge control model of Eq. (1) sets a cut-off critical thickness t_{CR} of the $\text{Zn}_{1-x}\text{Mg}_x\text{O}$ layer below which the 2DEG is not formed. The t_{CR} decreases from 38 to 1 nm as the x increase from 0.05 to 0.45. This behavior is similar to that of $\text{AlGaIn}/\text{GaIn}$ heterostructure.¹⁷

The good agreement between the theoretical prediction and experimental results allow us to infer the source of electrons in 2DEG. If ZnO layer was the origin of the 2DEG, then the carrier concentration would be independent of $\text{Zn}_{1-x}\text{Mg}_x\text{O}$ layer thickness as well as x composition. The 2DEG density is also not proportional to the $\text{Zn}_{1-x}\text{Mg}_x\text{O}$ layer thickness, which suggests that the effect of donors in

ZnMgO layer is not so important. The same conclusion is drawn by Tampo *et al.*¹⁶ that the mobile 2DEG charges originate from the donorlike surface states and oxygen vacancies are expected to be most possible candidates, which has a deep level of 0.7 eV below the conduction band of ZnO.¹⁸

We note that there is somewhat a large discrepancy in the sheet carrier concentration values obtained by C-V profiling (e.g., $1.23 \times 10^{12} \text{ cm}^{-2}$ for $\text{Zn}_{0.83}\text{Mg}_{0.17}\text{O}/\text{ZnO}$) and the calculated value ($2.02 \times 10^{12} \text{ cm}^{-2}$) using Eq. (1). This could be due to the depletion of a thinner ZnMgO barrier layer that led to an underestimation of the integrated carrier concentration of the C-V profiling. Additionally, the unintentional composition gradient during the growth of $\text{Zn}_{1-x}\text{Mg}_x\text{O}$ layer will cause a slight increase in the band gap energy and the x composition with the $\text{Zn}_{1-x}\text{Mg}_x\text{O}$ layer in our samples. This is possibly due to the composition-pulling effect, which has been also observed in the MBE growth for rich-Mg $\text{Zn}_{1-x}\text{Mg}_x\text{O}$ and also in $\text{In}_{1-x}\text{Ga}_x\text{N}$ growth.^{19,20}

This work was supported by the Singapore Agency for Science, Technology, and Research (A*STAR), under SERC Grant No. 0521260095 and Infuse Project No. I01-0911-06.

¹A. Tsukazaki, A. Ohtomo, T. Kita, Y. Ohno, H. Ohno, and M. Kawasaki, *Science* **315**, 1388 (2007).

²H. Tampo, H. Shibata, K. Maejima, A. Yamada, K. Matsubara, P. Fons, S. Kashiwaya, S. Niki, Y. Chiba, T. Wakamatsu, and H. Kanie, *Appl. Phys. Lett.* **93**, 202104 (2008).

³A. Tsukazaki, A. Ohtomo, M. Kawasaki, S. Akasaka, H. Yuji, K. Tamura, K. Nakahara, T. Tanabe, A. Kamisawa, T. Gokmen, J. Shabani, and M. Shayegan, *Phys. Rev. B* **78**, 233308 (2008).

⁴S. Sasa, M. Ozaki, K. Koike, M. Yano, and M. Inoue, *Appl. Phys. Lett.* **89**, 053502 (2006).

⁵M. Nakano, A. Tsukazaki, A. Ohtomo, K. Ueno, S. Akasaka, H. Yuji, K. Nakahara, T. Fukumura, and M. Kawasaki, *Adv. Mater. (Weinheim, Ger.)* **22**, 876 (2010).

⁶K. Koike, D. Takagi, M. Kawasaki, T. Hashimoto, T. Inoue, K. Ogata, S. Sasa, M. Inoue, and M. Yano, *Jpn. J. Appl. Phys., Part 2* **46**, L865 (2007).

⁷K. Koike, D. Takagi, M. Kawasaki, T. Hashimoto, T. Inoue, K. Ogata, S. Sasa, M. Inoue, and M. Yano, *Jpn. J. Appl. Phys.* **48**, 04C081 (2009).

⁸J. D. Ye, S. T. Tan, S. Pannirselvam, S. F. Choy, X. W. Sun, G. Q. Lo, and K. L. Teo, *Appl. Phys. Lett.* **95**, 101905 (2009).

⁹H. Tampo, H. Shibata, K. Maejima, A. Yamada, K. Matsubara, P. Fons, S. Niki, T. Tainaka, Y. Chiba, and H. Kanie, *Appl. Phys. Lett.* **91**, 261907 (2007).

¹⁰J. P. Ibbetson, P. T. Fini, K. D. Ness, S. P. DenBaars, J. S. Speck, and U. K. Mishra, *Appl. Phys. Lett.* **77**, 250 (2000).

¹¹I. P. Smorchkova, C. R. Elsass, J. P. Ibbetson, R. Vetury, B. Heying, P. Fini, E. Haus, S. P. DenBaars, J. S. Speck, and U. K. Mishra, *J. Appl. Phys.* **86**, 4520 (1999).

¹²O. Ambacher, J. Smart, J. R. Shealy, N. G. Weimann, K. Chu, M. Murphy, W. J. Schaff, L. F. Eastman, R. Dimitrov, L. Wittmer, M. Stutzmann, W. Rieger, and J. Hilsenbeck, *J. Appl. Phys.* **85**, 3222 (1999).

¹³L. Hsu and W. Walukiewicz, *J. Appl. Phys.* **89**, 1783 (2001).

¹⁴M. Yano, K. Hashimoto, K. Fujimoto, K. Koike, S. Sasa, M. Inoue, Y. Uetsuji, T. Ohnishi, and K. Inaba, *J. Cryst. Growth* **301-302**, 353 (2007).

¹⁵E. T. Yu, G. J. Sullivan, P. M. Asbeck, C. D. Wang, D. Qiao, and S. S. Lau, *Appl. Phys. Lett.* **71**, 2794 (1997).

¹⁶H. Tampo, H. Shibata, K. Maejima, T.-W. Chiu, H. Itoh, A. Yamada, K. Matsubara, P. Fons, Y. Chiba, T. Wakamatsu, Y. Takeshita, H. Kanie, and S. Niki, *Appl. Phys. Lett.* **94**, 242107 (2009).

¹⁷D. Jena, in *Polarization Effects in Semiconductors*, edited by C. Wood and D. Jena (Springer, New York, 2008), Chap. 2.2, p. 166.

¹⁸M. W. Allen, R. J. Mendelsberg, R. J. Reeves, and S. M. Durbin, *Appl. Phys. Lett.* **94**, 103508 (2009).

¹⁹Y. Nishimoto, K. Nakahara, D. Takamizu, A. Sasaki, K. Tamura, S. Akasaka, H. Yuji, T. Fujii, T. Tanabe, H. Takasu, A. Tsukazaki, A. Ohtomo, T. Onuma, S. F. Chichibu, and M. Kawasaki, *Appl. Phys. Express* **1**, 091202 (2008).

²⁰S. Pereira, M. R. Correia, E. Pereira, K. P. O'Donnell, C. Trager-Cowan, F. Sweeney, and E. Alves, *Phys. Rev. B* **64**, 205311 (2001).